Original Paper

Study of surface changes on industrial glasses with AFM, FE-SEM, EDX, SNMS and LM

Part 2. Surface changes by water drop etching, annealing at atmosphere and flame treatment

Chun Wang and Georg Krausch

Physikalische Chemie II, Universität Bayreuth, Bayreuth (Germany)

Edda Rädlein

Keramische Werkstoffe, Universität Bayreuth, Bayreuth (Germany)

Stephan Tratzky

SCHOTT-Rohrglas GmbH, Mitterteich (Germany)

Manfred Schramm

Bayerische Flaschen-Glashüttenwerke Wiegand Söhne GmbH Co. KG, Steinbach am Wald (Germany)

Andreas Weber

Nachtmann Bleikristallwerke GmbH, Weiden i.d. OPf (Germany)

One of the possible defects in sputter coating layers are cone shaped rods which originate from the float glass surface on the atmosphere side. The glass surface had been etched by wax-like corrosion droplets and holes were formed into the glass skin after washing. This results in inhomogeneity on the surface, which induces an inhomogenous deposition pattern of the material on the surface during the process of sputtering. In contrast, the tin bath side is shown to be an ideal coating surface without any inhomogeneity. In some cases however, it could not be bent above the glass transition temperature (T_g) in air due to formation of bloom patterns, which make the glass milky. Our studies revealed that phase separation is the ultimate cause of the observed bloom formation. In addition, sulphur flakes and needle-like nanocrystallites were detected on the tin bath side as well as hexagonal nanocrystallites on the atmosphere side of the annealed float glass.

It was also found that flame treatment of borosilicate and lead crystal glasses induced two changes on the glass surfaces. These are precipitation of evaporation products and phase separation beneath the glass skin. The samples were studied by a combination of field emission scanning electron microscopy (FE-SEM) with different accelerating voltages and atomic force microscopy (AFM).

1. Introduction

The nature of glass surfaces and their modification during different treatments are of considerable interest to glass science and its technological applications. In the previous paper [1] we have studied the surface changes in lead silicate glass tubing exposed to air and their relationship to the improved cutting behaviour of the tubing. Meanwhile the surface changes of soda-lime-silica glass bottles have been investigated. A glass skin was found to cover glass surfaces, which influences the corrosion behaviour significantly. The present work in the first part describes the float glass surface and its influence on the subsequent sputter coating as well as the surface changes induced by annealing. In the float process, molten glass floats on a molten tin bath, so that tin penetrates into the glass. As a result, the float glass has an atmosphere side and a tin bath side that feature many different properties with respect to chemical composition, mechanical abrasion and refractive indices etc. By annealing above the glass transition temperature, a wrinkling can appear on the surface of the glass called "bloom". Various studies have been carried out on float glass in the past, most of which can be categorized into three groups:

Received 24 June 2004.

Presented in German at: 77th Annual Meeting of the German Society of Glass Technology (DGG) on 28 May 2003 in Leipzig (Germany).

corrosion of float glass in humidity and in water along with composition changes during the corrosion process [2 to 8]; characterization of tin in float glass before and after annealing above T_g [9 to 16]; other studies on float glass surfaces [17 to 20]. Up to now, few papers have described the direct influence of the float glass surface on the sputter coating layers. This study was motivated by industry's demand to study the surface properties on both sides of the float glass and to explain some of the defects of the coating layers on float glass.

In the second part of this work, flame induced surface changes of glass will be discussed. Flaming is often used as a postproduction treatment method in order to make glass articles suitable for different applications. Examples include, remelting glass tubing into bottles or ampoules; melting glass surfaces to remove the pressing burrs and cold waves and rounding the sharp cutting edges. Flame induced surface change is one of the least experimentally and theoretically developed problems, which can readily be explained by the fact that the final products draw little attention from researchers. Still, in industry, where the maintenance of a stable level of quality is crucial during the production process, it is important to have an understanding of these occurring changes. Besides, the results of this study have not only industrial benefits but have equal importance for the glass science in general.

2. Experimental

2.1 Samples

Commercial soda-lime-silica float glass with a thickness of 1.6 mm was used in the first part of this study. A (5 × 10) cm^2 sized sheet of this glass was put onto ceramic supports in an electric furnace (Nabertherm) and heated at 650 °C under ambient conditions. After annealing for 1 h, the sheet was quenched to room temperature and stored in air for further investigation. Another sample, a washed float glass, was taken directly from the production process prior to sputter coating. Finally a sample of float glass with an ITO monolayer, which is an intermediate product of the coating process, was investigated.

The second part of the study focused on borosilicate ampoules, which were remolten from tubing and featured defective white spots on the inner wall. The third part of the study examined a lead crystal fire polished bowl which underwent acid polishing as the last finishing process.

2.2 Analytical techniques

The surface, near surface and bulk structures of the samples were investigated by light microscopy (LM, Axiovert, Carl Zeiss Jena GmbH, Jena (Germany)), by height mode atomic force microscopy (AFM, NanoScope Dimension, 3100, Digital Instruments, Santa Barbara, CA (USA)) and by field emission scanning electron microscopy (FE-SEM, LEO 1530, Carl Zeiss NTS Inc., Oberkochen (Germany)). The FE-SEM is equipped with three detectors: a) The Inlens detector collects the secondary electrons originating directly from the spot centre. Through application of accelerating voltages between 0.5 and 2 kV the surface morphology of samples can thus be elucidated. b) The SE 2 detector collects the secondary electrons from a deeper region underneath the surface. For this means, higher accelerating voltages of above 5 kV are employed to image the near surface structure. c) The Rutherford backscattering detector (RBSD) collects the back scattered electrons (at a voltage between 7 and 20 kV) and reveals material contrast images. The chemical compositions of the samples were determined with energy dispersive X-ray spectrometry (EDX, INCA 400, Oxford Instruments, Concord, MA (USA)) equipped on the FE-SEM instrument. The element depth profiles of the samples were recorded by using secondary neutral mass spectrometry (SNMS, INA 3, Leybold AG, Köln (Germany)). Samples studied with FE-SEM were coated with carbon prior to examination. The AFM measurements were carried out on bare glass surfaces at ambient conditions.

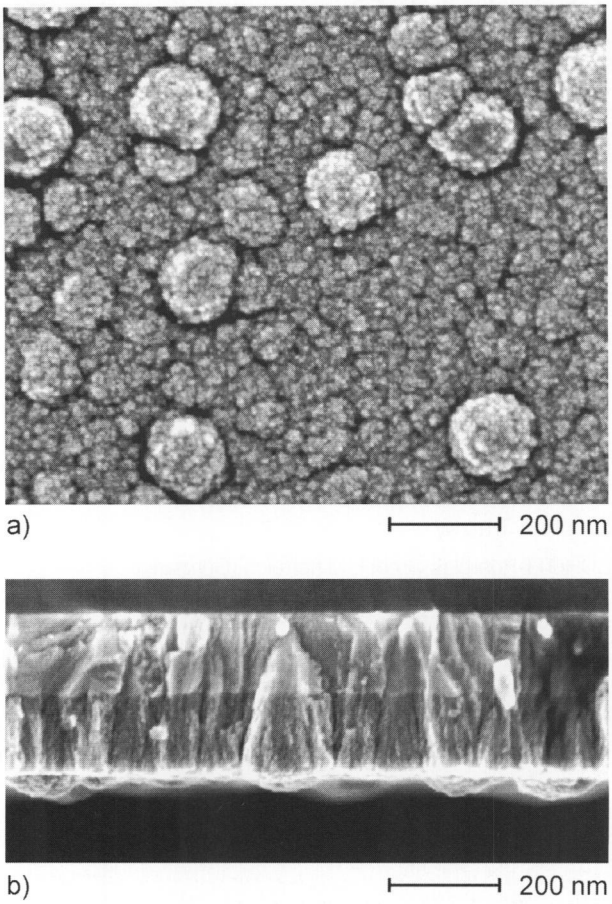

Figures 1a and b. FE-SEM micrographs (Inlens, 1 kV) at an intermediate product step of an electrochromic mirror with two sputtered layers on the atmosphere side of float glass; a) surface view of the top layer, b) cross-sectional view of the two layers.

3. Results and discussion

3.1 Coated and heat-treated float glass

In sputter coated multilayer systems, cone shaped rods can disturb the stack of layers and consequently impair the physical properties of the whole system. Figures 1a and b show a top view as well as a sectional view of the rods. It can be seen that the featured rods have a different density

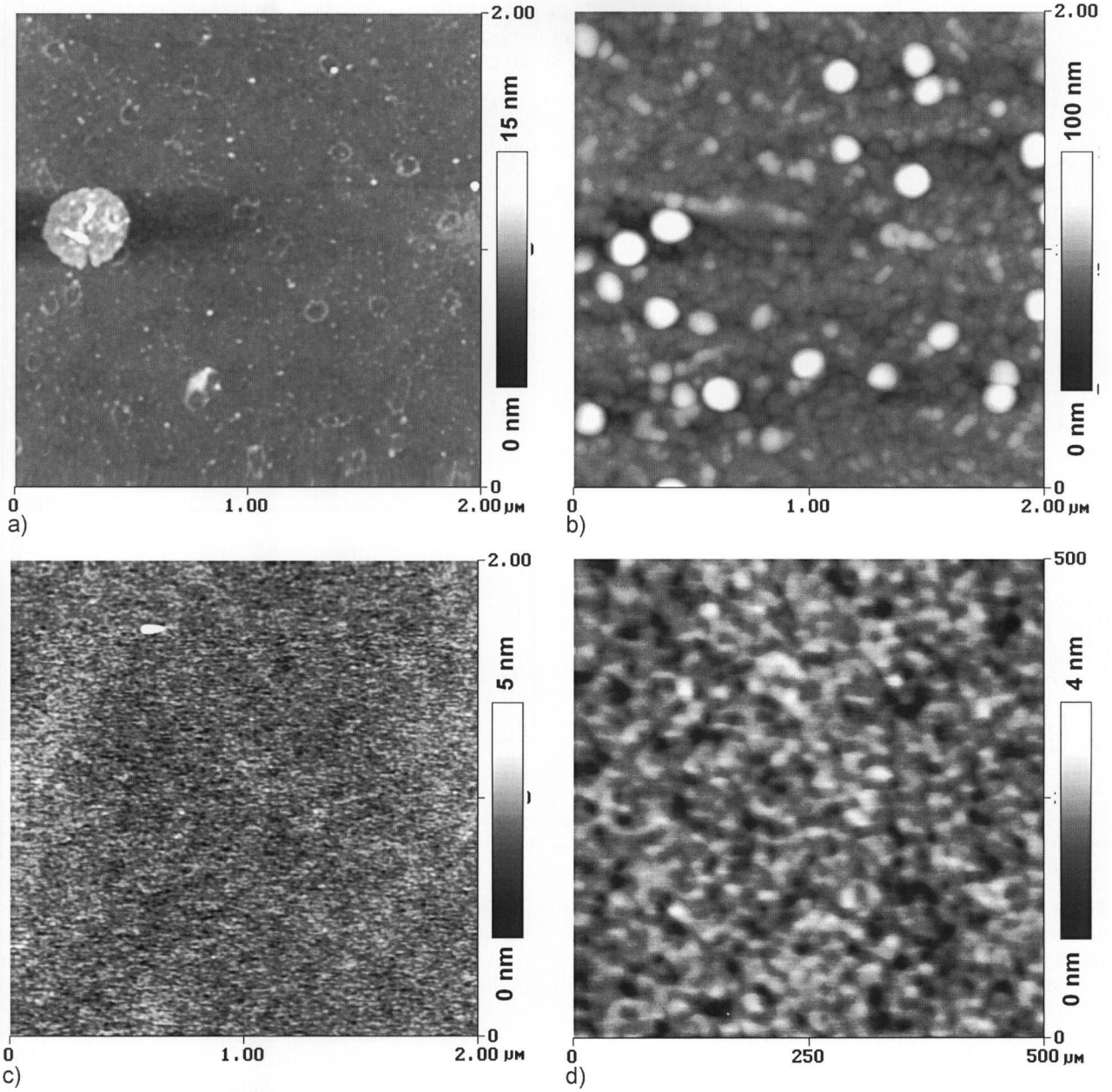

Figures 2a to d. AFM images of both sides of float glass after washing with water as well as the first ITO layer on atmosphere side; a) atmosphere side showing the glass skin etched by water drops, b) sputter coating ITO layer, c) and d) tin bath side on different scales.

from the surrounding continuous area. They originate from the glass surface, enlarge gradually during further sputter coating and pass through one layer into another. The rods protrude from the surface as much as 100 nm and bridge between individual layers, thus mixing electrical and other physical properties of neighbouring layers. In order to study the origin of the growth of rods, both sides of float glass were examined after washing and prior to coating. Also investigated was a primary indium tin oxide (ITO) layer, sputtered onto the atmosphere side of float glass. Figures 2a to d exhibit the results of the AFM investigation. Figure 2a shows the washed atmosphere side of float glass. It can be seen from the image that holes are scattered statistically on the surface and are surrounded by a slightly elevated rim. We assume that these features stem from the remaining traces of wax-like droplets, which were removed by the washing process. The observed hole-like structures only occur when the surface is covered by an SiO_2-rich skin layer, which was postulated earlier in [1]. Similar studies on glass surfaces that exhibit wax-like droplets also revealed holes after the washing process [21]. The morphology of these holes was found to be quite similar to those found in our investigation. However, in these studies there is no mention of an SiO_2-rich skin and its role in hole formation. Figure 2b shows the ITO layer. The bright spots are the cone shaped rods at their initial formation stage and their sizes and distribution pattern are comparable with the traces of water drops in figure 2a. If a flat surface is subjected to the sputtering process, the deposited particles gather primarily on the protruding objects and consequently result in zones in the coating layer that are characterized by higher densities and faster growth. Our investigation indicates that the

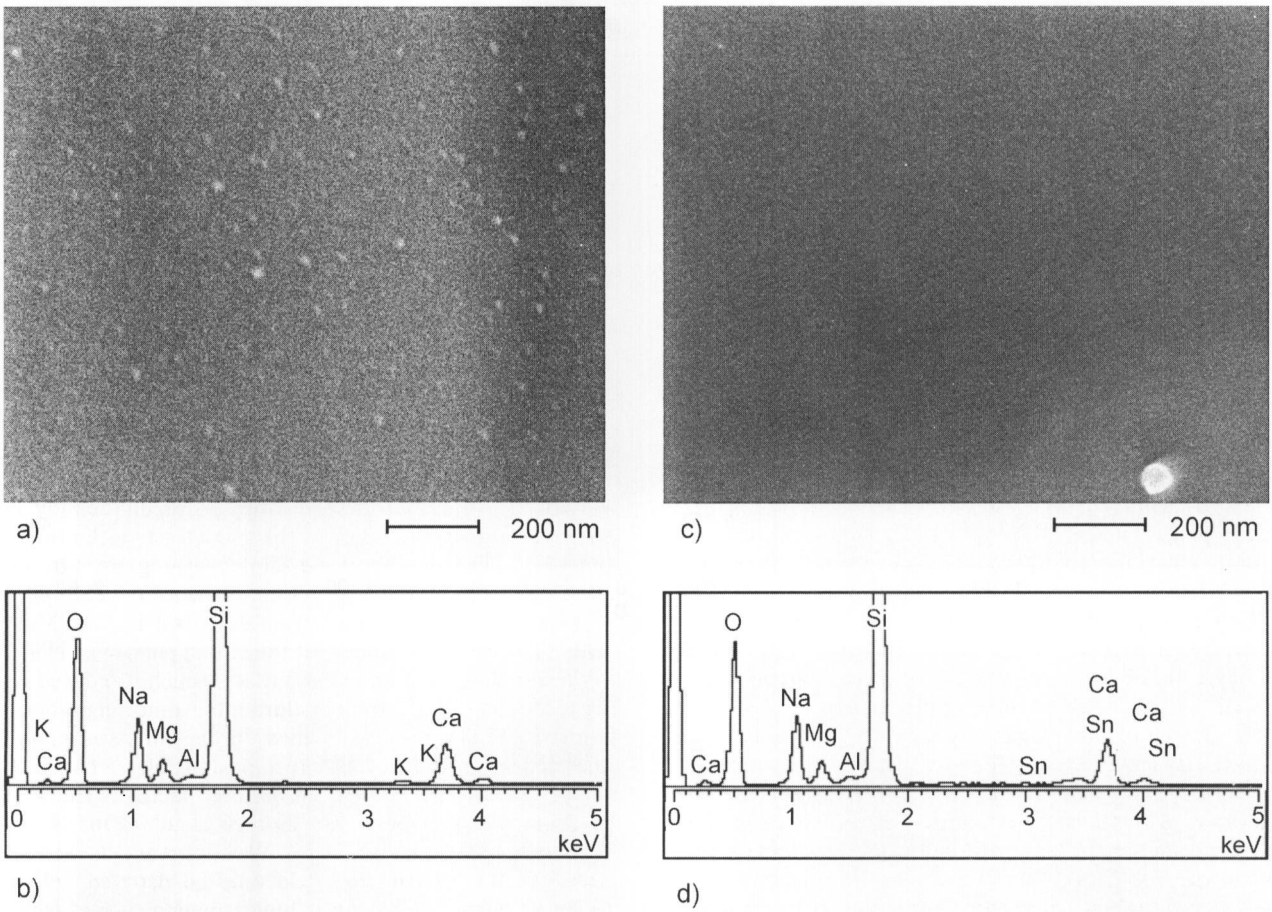

Figures 3a to d. FE-SEM micrographs (Inlens, 1 kV) and the corresponding EDX spectra (20 kV, scanned for 600 s) of float glass two weeks after washing with water; a) and b) atmosphere side, c) and d) tin bath side.

slightly elevated rims of the etched holes in figure 2a are probably responsible for the growth of the observed rods. Based on hole size two different morphologies of rods can be distinguished. Holes with rather small diameters result in rods that feature a protruding top, whereas holes of larger diameter lead to rods with depressed tops. Both types of structure could be observed in one of our unpublished works. Figures 2c and d show the tin bath side of float glass on different scales. Figure 2c illustrates the homogeneity of the surface with no visible marks of corrosion. Magnified by a factor of 4 (figure 2d) fine-grain nanostructures with a size of about 30 nm become apparent. Measurements of the roughness of a (2 × 2) μm^2 sample of the surface resulted in an RMS (root mean square) value of 0.30 nm. The tin bath side changes scarcely when exposed to humid air for a long time [2 to 4] and there are no visible traces of water drops and no sputtering defects on it. The two different sides of float glass can be distinguished with EDX equipped with FE-SEM. Figures 3a to d show the morphologies and the corresponding EDX spectra of the atmosphere and bath sides, respectively. From figure 3a one can observe droplet-like corrosion products. The corresponding spectrum (figure 3b) shows the chemical surface components. As expected no Sn peak is detected on this side. In contrast, the morphology on the tin bath side (figure 3c), when examined under the same magnification as the atmosphere side, is devoid of any features and is characterized by a high degree of homogeneity. The corresponding spectrum (figure 3d) displays distinct Sn peaks. From the obtained spectral data and the morphological images one can differentiate clearly between the atmosphere side and the bath side. The EDX values from figures 3b and d regarding the chemical composition of the surfaces are listed in table 1.

Due to production requirements, float glass sometimes needs to be formed into concave or convex shapes by thermal treatments above T_g. Frequently, these treatments induce the formation of bloom patterns which causes the glass to become murky eventually leading to a loss of transparency [9 to 14]. In order to understand the features of the annealed float glass surface and their influence on the sputter coating layers, a thermal treatment experiment was carried out in the laboratory. For that purpose, a float glass sample (5 × 10) cm^2 × 1.6 mm, bath side on top) was put on two supporting ceramic pieces in an electric furnace and heated at 650 °C in ambient conditions for 1 h and then was quenched to room temperature in air. During the annealing process the glass sample formed into a concave shape due to gravity. One side looked murky and rough whereas the other side appeared brilliant and smooth. Figures 4a to c exhibit the outmost surface morphologies from both sides by using lower accelerating voltage (1 kV) and the topography detector (Inlens) of FE-SEM. The survey micrograph of the tin bath side in figure 4a shows the previously mentioned bloom patterns and additional sulphur containing flakes which can primarily be found at the centres of convergent bloom ripples. Since the tin bath side of new float glass is devoid of sulphur within the first few µm of depth [22],

Table 1. Elements in atom% detected by EDX on both sides of float glass at 20 kV and scanned for 600 s

	O	Na	Mg	Al	Si	K	Ca	Sn
atmosphere side	62.35	7.45	1.95	0.15	25.00	0.14	2.97	
tin bath side	61.81	7.48	1.96	0.19	25.14		5.15	0.26

Table 2. Elements in atom% detected by EDX on annealed bath side of float glass at 7 kV and scanned for 100 s

	O	Na	Mg	Si	Ca	Sn
spectrum 1	67.88	2.17	1.62	25.85	1.61	1.16
spectrum 2	66.09	1.85	1.74	27.69	2.64	

sulphate stemming from the bulk must be involved in the redox processes leading to the observed bloom structures. During annealing, sulphur containing species from the bulk can diffuse to the surface and finally are oxidized to sulphates or sulphides on the glass surface. The result of this process is illustrated by the enlarged surface image shown in figure 4b, which displays numerous needle-like nanocrystallites, which are the ultimate cause of the sputtering defects. In one of our earlier investigations, it has been observed that many needle-like flat plateau features appeared in the annealed coating layers. At the time, it was not known however, whether the defects were induced by errors originating from the sputtering technique or by the imperfection of the glass surface. From our current investigation it can be deduced that the defects are neither sputtering errors nor surface imperfection, but instead are the immediate result of the annealing treatment.

The original bath side can be as homogenous as shown in figure 2c and figure 3c, but during annealing some species can diffuse out of the bulk to form objects of certain shape on the surface. This process may even take place at temperatures below T_g. The mobility of glass components below and above the glass transition temperature is described in the literature [23]. The annealed atmosphere side has no bloom pattern at all when examined on the µm scale but shows hexagonally shaped nanocrystallites instead of the needle-like crystallites found on the bath side (figures 4b and c). Consequently, it may be concluded that annealing in air can result in unexpected inhomogeneities on both sides of float glass, which subsequently can result in poor adhesion and poor quality of the coating layers on the glass surface. Possible methods in order to eliminate the annealing-induced inhomogeneities are currently under investigation.

If the accelerating voltage of the FE-SEM is increased to 7 kV and a material contrast detector (RBSD) added, the bloom pattern in figure 4a (1 kV, Inlens) appears more clearly than in figure 5a. Additionally, the sulphur flakes are not so clearly visible as in the corresponding micrograph of figure 4a and the needle-like crystallites can not be observed anymore. The bloom pattern consists of brighter and darker stripes that exhibit a period of about 1 µm. The contrast of bright and dark that can be observed in the stripe sequences stems from the various atomic species and their differences in atomic weight. As a result, lighter elements such as silicium yield a weaker signal (darker) whereas heavier elements such as tin result in a stronger signal (brighter). Moreover, featured stripes are oriented predominantly in one direction which stands in sharp contrast to the rather chaotic-like distribution of the sulphur aggregates. The observed stripe pattern is a direct consequence of the typical phase separation phenomenon as described in [24]. Most studies [9 to 14] confirmed that the bloom pattern is related to the enrichment of Sn at the surface, which is induced by the oxidation of Sn^{2+} to Sn^{4+} during the annealing process in air. The EDX results obtained during our investigation show the same tendency. Before annealing, all tin bath surfaces of float glass taken from different factories show an Sn content in the range of 0.23 to 0.28 at.%. One of the measurements is listed in table 1. Without previous thermal treatment the Sn content could only be detected with a higher voltage of 20 kV and a long scanning time of 600 s. However, after the annealing process, the Sn content could already be detected with a lower voltage of 7 kV and a significantly shorter scanning time of 100 s. The Sn content in this case reached values above 1 atom% as shown in table 2. In conclusion, after annealing an Sn enrichment of the surface takes places. In a similar study of another research group [11 and 12], it was pointed out that the formation of the bloom pattern was due to a different thermal expansion coefficient of the topmost Sn enriched layer compared to that of the bulk glass. As a consequence, it was postulated that wrinkling of the tin bath side occurs. However, the micrograph in figure 5a shows that the ripples are formed from different materials (RBSD) and that the pattern is located in deeper layers of the outmost surface (higher voltage). This corresponds to most SNMS depth profiles where the maximum enrichment of the Sn signal is at a position of 50 to 100 nm below the surface.

Hence, it is reasonable to believe that the bloom pattern is the consequence of a phase separation during which an Sn-rich phase in the surrounding SiO_2-rich matrix is created. This phase separation occurs underneath the glass skin. In order to reinforce the suggested phase separation, the EDX measurements were carried out carefully on various darker as well as brighter stripes. Most results show that the tin content of the brighter stripes is higher than that of the darker stripes and that in extreme cases, there is no tin signal on the darker stripe at all. Figures 5b and c show the FE-SEM micrographs and the corresponding spot EDX spectra. The associated data is listed in table 2. In conclusion, all of the obtained evidence indicates that the bloom pattern is ultimately formed by a phase separation process of the glass near surface which is due to chemical

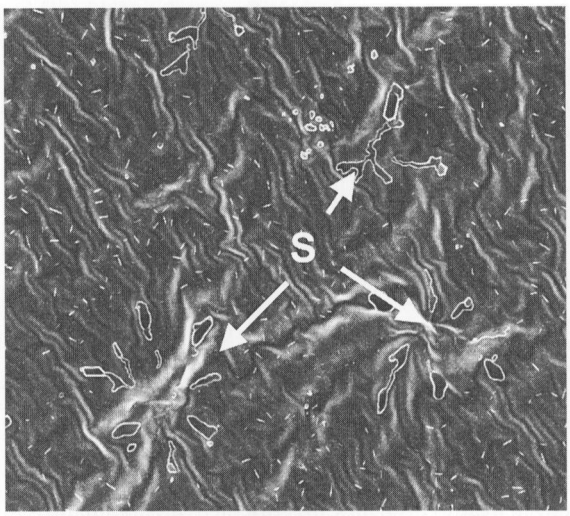

a) 10 µm

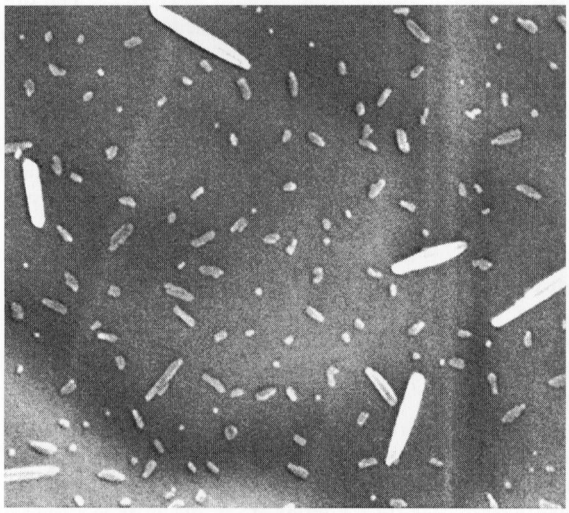

b) 500 nm

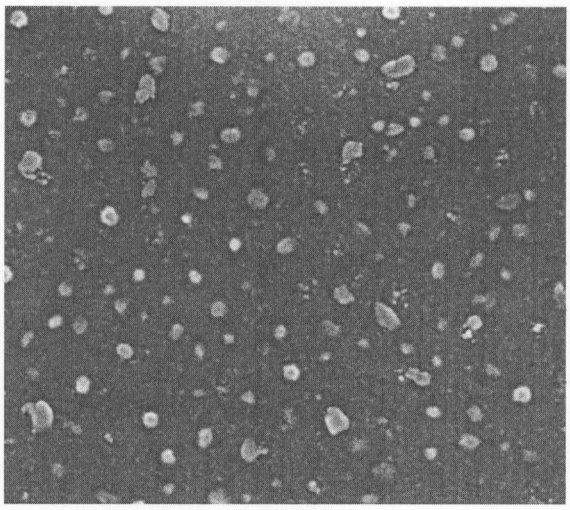

c) 500 nm

Figures 4a to c. FE-SEM micrographs (Inlens, 1 kV) of the outmost surface morphologies of float glass on both sides after annealing at 650 °C for 1 h in air; a) overview showing the bloom pattern and additional sulphur flakes, b) needle-like nanocrystallites on the tin bath side and c) hexagonally shaped nanocrystallites on the atmosphere side.

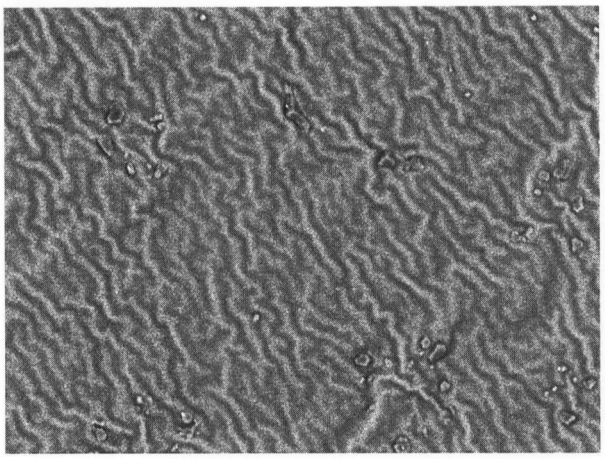

a) 10 µm

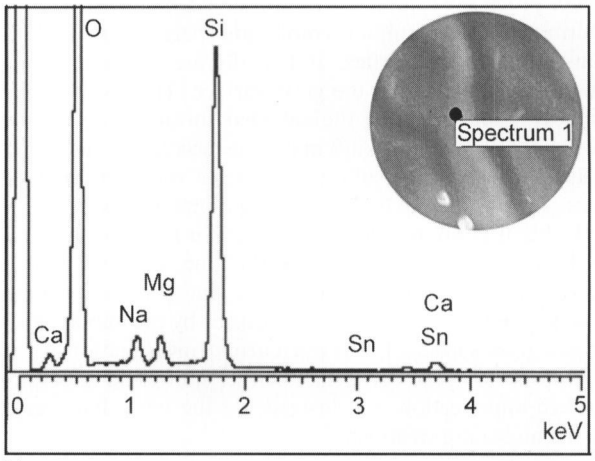

b)

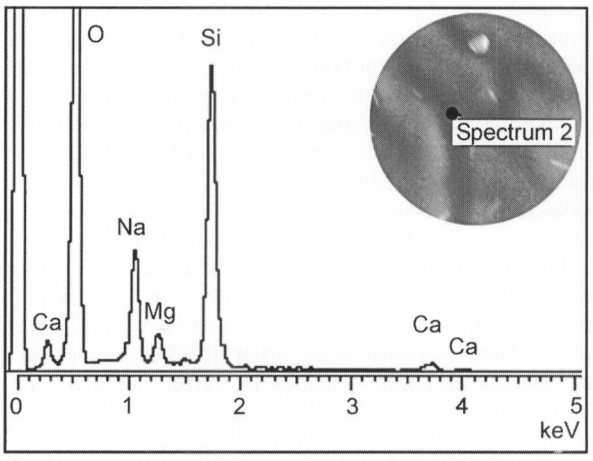

c)

Figures 5a to c. Material contrast FE-SEM micrograph (RBSD, 7 kV) (figure a), and EDX spot analysis of the brighter stripes (figure b) and the darker stripes (figure c), which show the ripple-like phase separation on the bath side of the annealed float glass.

composition changes during thermal treatment of the float glass [9 to 13]. Here we show for the first time that the bloom is a phase separation phenomenon.

3.2 Flame treated borosilicate and lead crystal glasses

There is a wide temperature range from 600 to 2000 °C at different positions within the flame. Consequently, numerous features can be developed on the flame treated glass surface. Here we discuss only two phenomena: evaporation and phase separation.

Figures 6a to c display some evaporation products observed on borosilicate ampoules, which were formed by remelting of tubing with fire. At the remolten bottom and the adjacent side wall at several millimetres from the bottom, there is no detectable feature at all, even if the articles were exposed to air for a long time. So the remolten area is ion-poor, similar to a quartz glass, which can sustain the attack of the surrounding media. At the position of about 1 cm from the bottom, different crystalline aggregates can be observed due to the remelting in different media. Based on the EDX analysis and the crystal forms it is suggested that the multilayer crystals in figure 6a may be the chain-like or ring-like crystal of $Na_3(B_3O_6)$, the sharp cornered crystals in figure 6b may be NaF or CaF_2 and the square shaped thin crystals may be NaCl as shown in figure 6c. However, the exact chemical compositions and the crystal structures of the aggregates are out of the scope of this work. In industry, the evaporation products worsen the quality of glass articles.

The flame induced phase separation can be best demonstrated on a fire polished lead crystal bowl surface. The treated area looks black or golden and brilliant. Under an optical microscope some yellow flowers, dark spots etc. were observed at different positions. Figures 7a and b present two examples of the optical micrographs. The AFM measurements on the spots show less features than detected by the optical microscope. A typical morphology revealed by AFM is presented in figure 8a, it resembles local contractions. The FE-SEM measurement on the same place as examined with AFM showed another feature. The whole surface is covered with spheres in the sizes of 100 nm or less, arranged in a monolayer. There are no spots as shown in the LM pictures (figures 7a and b) and there is no pattern similar to the AFM image (figure 8a). Then the sample was measured with FE-SEM by adjusting the accelerating voltages as well as the working distances and by inserting various detectors. One series of the measurements is listed in figure 8b. At 1 kV the micrograph shows the same pattern as the one revealed with AFM, at 2 kV the surface feature is obscure and some spheres appear, at 3 and at 5 kV very clear spheres are observed. A phase separation has taken place beneath the glass skin. The schematic drawing of this phenomenon is presented in figure 8c. The element depth distribution of the sample surface was studied with SNMS.

Figure 9 displays a strong peak of Pb near the surface in the depth of about 50 nm (similar to the tin peak in the profile of the annealed tin bath side of float glass [11]). The enrichment in Pb may be induced by the reduction of Pb^{2+} to Pb^0 during the reducing flame treatment (CO). The result of SNMS depth profile corresponds well with the microscopy investigations. The FE-SEM survey micrograph (RBSD, 5 kV) in figure 10 shows more general features of the fire polished lead crystal glass surface beneath a glass skin. The brighter spheres should be the isolated Pb-rich domains because of the stronger contrast of heavier Pb

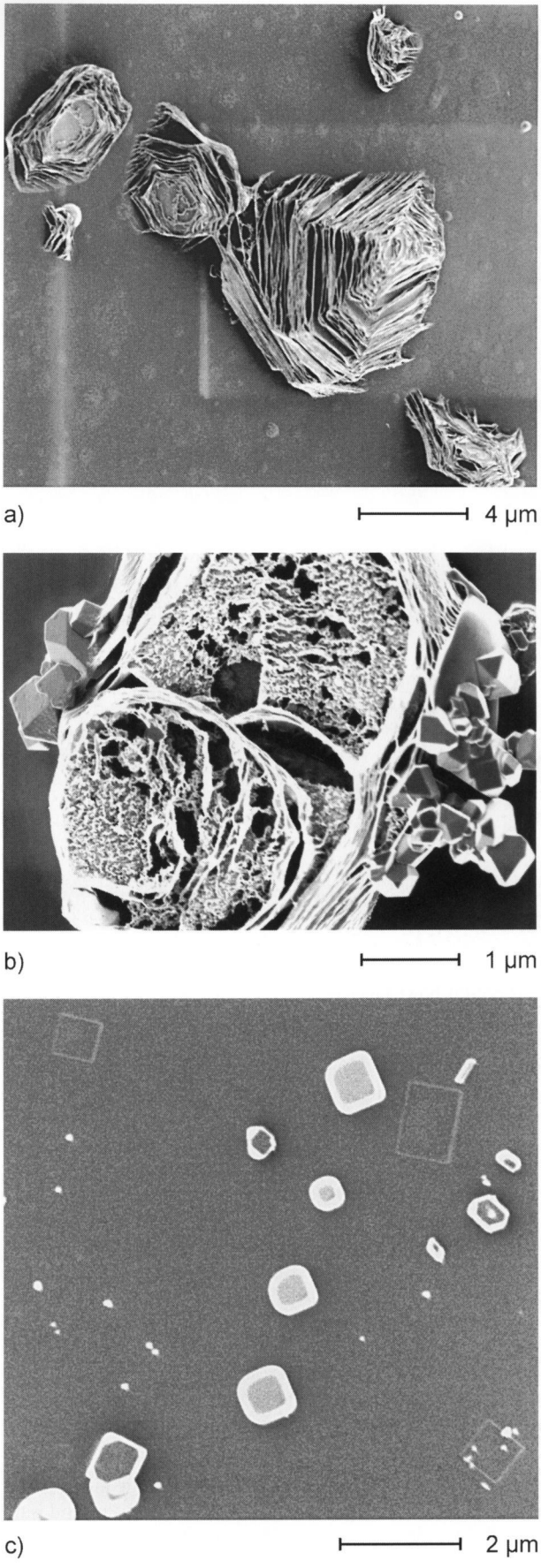

Figures 6a to c. FE-SEM micrographs (Inlens) of evaporation products condensed on the ampoules inner surfaces; a) at 0.5 kV, b) and c) at 1 kV.

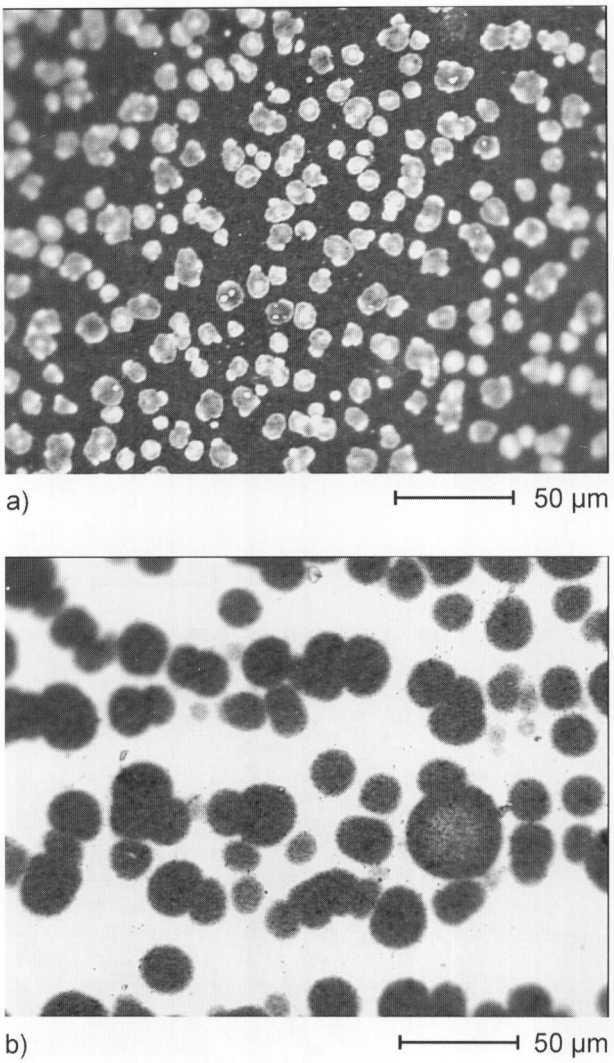

Figures 7a and b. Optical microscopic pictures of a fire polished lead crystal bowl surface.

compared with the SiO_2-rich matrix. The spheres assemble into different aggregates with different sizes and different densities, which may result in patterns in LM micrographs as shown in figures 7a and b of the same surface area. The AFM measurement in figure 8a shows yet another morphology as described above. Consequently, these results perfectly illustrate that it is crucial to combine different characterization methods in order to avoid a misinterpretation of the real structure. Additionally, the fire polished lead crystal bowl was polished with acid solution. The surface of the final product is very flat and maintains stable towards the corrosion in moist air for a long time. It is possible that the ions near the glass surface have been leached out and leave a thicker SiO_2-rich layer which protects the glass from the attack of the surrounding media.

Flame induced phase separation has not only been observed on fire polished lead crystal bowls but also on the remolten mouth rim and stem base of lead crystal and barium silicate wine cups and on the remolten mouth rim of a borosilicate coffee pot. It is the cause of the visible local cloudiness of glass articles after certain cycles in dishwashers [25]. The phase separation phenomenon in glasses has been known for a long time already, e.g. in barium boro-

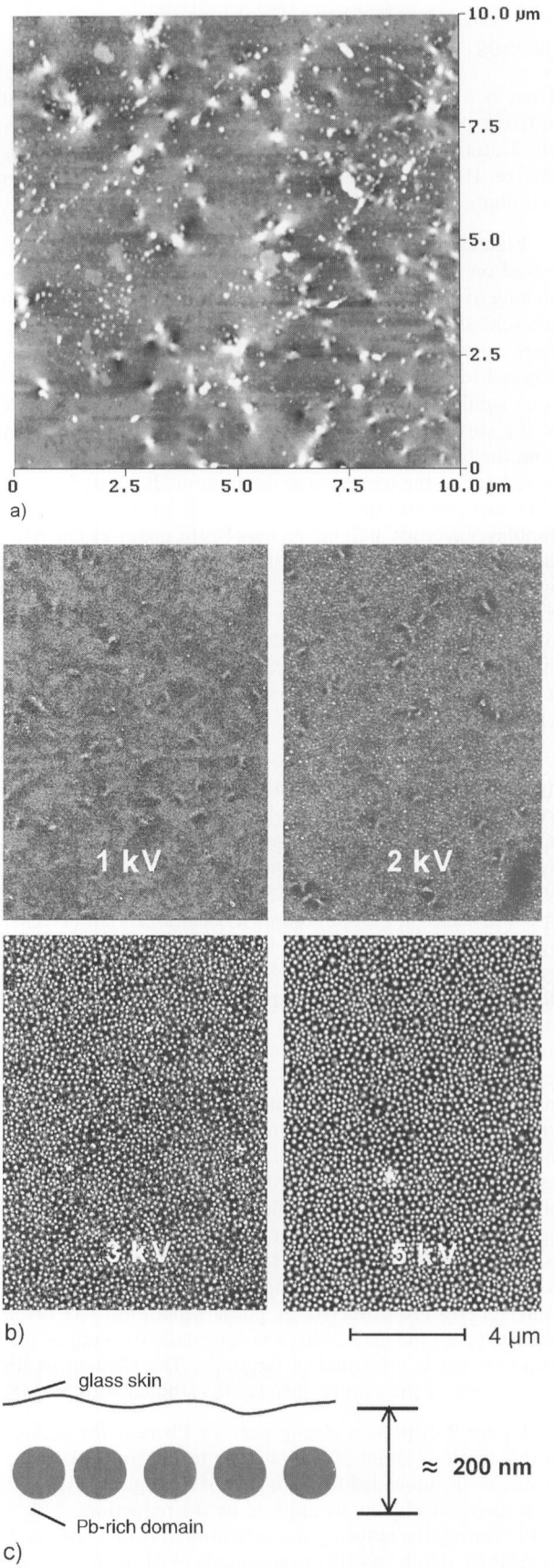

Figures 8a, b and c. AFM image of the fire polished lead crystal bowl surface (figure a); FE-SEM micrographs (Inlens, with different voltages) of the same sample as in figure 8a (figure b); and schematic drawing of the phase separation beneath a glass skin (figure c).

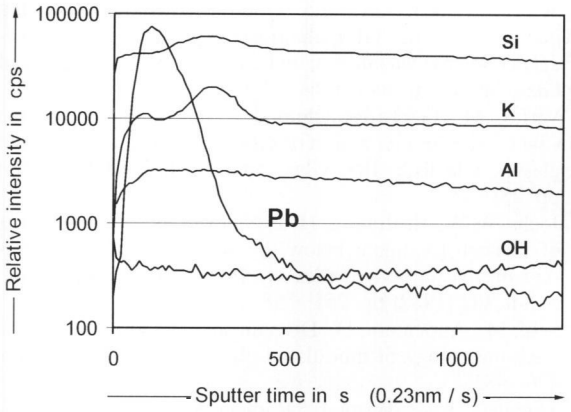

Figure 9. SNMS depth profiles of the fire polished lead crystal glass surface showing a strong enrichment of lead in the near surface region.

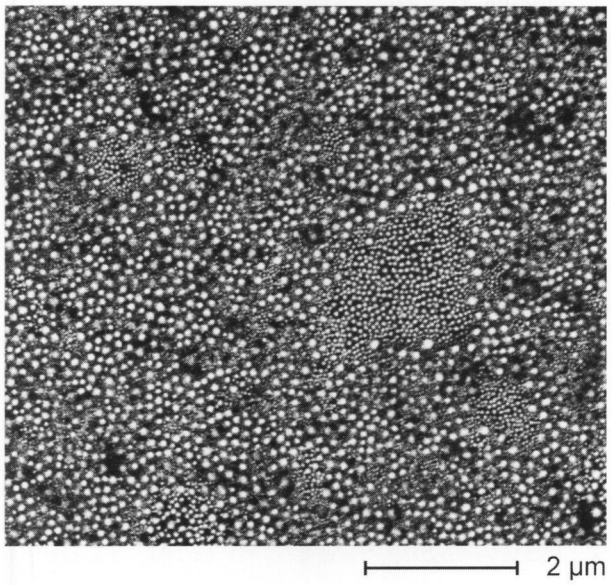

Figure 10. Survey view of the fire polished lead crystal glass surface showing different sphere aggregates (material contrast FE-SEM micrograph at 5 kV, with RBSD).

silicate glass, lithium silicate glass, bioglass ceramics etc. Many glasses have the tendency to show phase separation as a direct consequence of thermodynamics [26]. In contrast, this study focuses on surface treatment induced composition changes that are followed by phase separation through chemical reactions of the surrounding media with the treated glass surface, like oxidation on the tin bath side of float glass and reduction on the fire polished lead crystal glass surface.

4. Conclusion

This study has shown that traces of water drops on the atmosphere side of the washed float glass are the origin of the growth of cone shaped rods as defects in sputter coating layers. Annealing the float glass above T_g in an oxidizing atmosphere gives rise to ripple-like phase separations (blooms) of the Sn-rich phase in the glass matrix on the tin bath side. During annealing, sulphur containing species can diffuse out of the bulk and form e. g. sulphates or sulphides (e.g. $CaSO_4$, Na_2SO_4) on the surface. Furthermore, there are needle-like nanocrystallites on the bath side and hexagonally shaped nanocrystallites on the atmosphere side of the annealed float glass, which result in defects of the coating layers. After flame treatment two additional features appear on glass surfaces, namely phase separation and evaporation products, which affect heavily the quality of the final products.

Postproduction treatments such as flaming are important techniques to broaden the use of glass articles, but one must also take into account the possible negative side effects.

*

Financial support from Freistaat Bayern through WOPAG (Werkstoffverbunde und Oberflächenveredelte Produkte aus Glas) is gratefully acknowledged.

5. References

[1] Wang, C.; Häfner, W.; Krausch, G. et al.: Study of surface changes on industrial glasses with AFM, FE-SEM, EDX, SNMS and LM. Pt. 1. Glass skin and corrosion. Glass Sci. Technol. **77** (2004) pp. 103–110.

[2] Ray, A.; Wuhrer, R.; Jacob, L.: Tin's beneficial effect in aqueous corrosion of float glass. In: Proc. 6th International Glass Processing Days, Tampere 1999. Pp. 222–223.

[3] Bange, K.; Anderson, O.; Rauch, F. et al.: Multi-method characterization of soda-lime glass corrosion. Pt. 1. Analysis techniques and corrosion in liquid water. Glastech. Ber. Glass Sci. Technol. **74** (2001) pp. 127–141.

[4] Bange, K.; Anderson, O.; Rauch, F. et al.: Multi-method characterization of soda-lime glass corrosion. Pt. 2. Corrosion in humidity. Glass Sci. Technol. **75** (2002) pp. 20–33.

[5] Feldmann, M.; Weißmann, R.: Initial stages of float glass corrosion. J. Non-Cryst. Solids **218** (1997) pp. 205–209.

[6] Matoušek, J.; Maryška, M.; Helebrant, A.: Cation concentration profiles in float glass surfaces during corrosion in aqueous solution. Glastech. Ber. Glass Sci. Technol. **69** (1996) pp. 7–11.

[7] Richardson, R. M.; Dalgliesh, R. M.; Brennan, T. et al.: A neutron reflection study of the effect of water on the surface of float glass. J. Non-Cryst. Solids **292** (2001) pp. 93–107.

[8] Grimal, J. M.; Chartier, P.; Lehuédé, P.: X-ray reflectivity: a new tool for the study of glass surfaces. J. Non-Cryst. Solids **196** (1996) pp. 128–133.

[9] Takeda, S.; Akiyama, R.; Hosono, H.: Precipitation of nanometer-sized SnO_2 crystals and Sn depth profile in heat-treated float glass. J. Non-Cryst. Solids **311** (2002) pp. 273–280.

[10] Takeda, S.; Akiyama, R.; Hosono, H.: Formation of nanometer-sized SnO_2 colloids and change in Sn-depth concentration profile in float glass induced by oxygen diffusion from atmosphere at temperatures above T_g. J. Non-Cryst. Solids **281** (2001) pp. 1–5.

[11] Moseler, D.; Heide, G.; Frischat, G. H.: Atomic force microscope study of the topography of float glasses and a model to explain the bloom effect. Glass Sci. Technol. **75** (2002) pp. 174–183.

[12] Frischat, G. H.; Müller-Fildebrandt, C.; Moseler, D. et al.: On the origin of the tin hump in several float glasses. J. Non-Cryst. Solids **283** (2001) pp. 246–249.

[13] Williams, K. F. E.; Johnson, C. E.; Greengrass, J. et al.: Tin oxidation state, depth profiles of Sn^{2+} and Sn^{4+} and oxygen diffusivity in float glass by Mössbauer spectroscopy. J. Non-Cryst. Solids **211** (1997) pp. 164–172.
[14] Williams, K. F. E.; Johnson, C. E.; Nikolov, O. et al.: Characterization of tin at the surface of float glass. J. Non-Cryst. Solids **242** (1998) pp. 183–188.
[15] Wang, T. J.; Zhang, H., Zhang, G. et al.: Computer modeling of satellite peak in tin profile of float glass. J. Non-Cryst. Solids **271** (2000) pp. 126–136.
[16] Lamouroux, F.; Can, N.; Townsend, P. D.: Ion beam analysis of float glass surface composition. J. Non-Cryst. Solids **212** (1997) pp. 232–242.
[17] Townsend, T. D.; Can, N.; Chandler, P. J. et al.: Comparisons of tin depth profile analyses in float glass. J. Non-Cryst. Solids **223** (1998) pp. 73–85.
[18] Deubener, J.; Brückner, R., Hessenkemper, H.: Nucleation and crystallization kinetics on float glass surfaces. Glastech. Ber. **65** (1992) pp. 256–266.
[19] Gorokhovsky, A.; Matazov, K.; Escalante-Garcia, J. I.: Modification of the float-glass surface by treatment with urea aqueous solution. J. Non-Cryst. Solids **291** (2001) pp. 43–49.
[20] Oakley, D. R.: An empirical study of the effect of stressed area on the strength of float glass surfaces. J. Non-Cryst. Solids **196** (1996) pp. 134–138.
[21] Schwarzenbach, M. S.: Oberflächencharakterisierung pharmazeutischer Glasbehältnisse und Messung verschiedener Wechselwirkungen zwischen Interferon α-2a and Glas. Basel University, Diss. 2001.
[22] Verità, M.; Geotti-Bianchini, F.; Guadagnino, E. et al.: Chemical characterization of the bottom side of green float glasses. Glastech. Ber. Glass Sci. Technol. **68 C1** (1995) pp. 251–258.
[23] Jochs, W. W.; Hoffmann, H. J.; Neuroth, N. M.: The effects of thermal treatment below the glass transition temperature on the refractive index of optical glass. J. Non-Cryst. Solids **102** (1988) pp. 255–258.
[24] Seul, M.; Andelman, D.: Domain shapes and patterns: The phenomenology of modulated phases. Sci. **267** (1995) pp. 476–483.
[25] Martinek, K.-P.; Wang, C.; Rädlein, E. et al.: Local clouding of glass after mechanical automatic dishwash. Glass Sci. Technol. Accepted for publication.
[26] Vogel, W.: Microphase separation in glasses. In: Bach, H.; Krause, D. (eds.): Analysis of the composition and structure of glass and glass ceramics. Berlin et al.: Springer, 1999. Pp. 477–491.

E604P002

Contact:

Dr. Chun Wang
Lehrstuhl für Physikalische Chemie II
Universität Bayreuth
Universitätsstraße 30
D-95440 Bayreuth

E-mail: chun.wang@uni-bayreuth.de